

# Formaldehyde-Free Prorobitenidin/Profisetinidin Tannin/Furanic Foams Based on Alternative Aldehydes: Glyoxal and Glutaraldehyde

X. Li<sup>1</sup>, A. Pizzi<sup>\*1,2</sup>, X. Zhou<sup>\*3</sup>, V. Fierro<sup>4</sup> and A. Celzard<sup>4</sup>

<sup>1</sup> ENSTIB-LERMAB, University of Lorraine, 27 rue Philippe Séguin, BP1041, 88051 Epinal cedex 9, France

<sup>2</sup> Dept. of Physics, King Abdulaziz University, Jeddah, Saudi Arabia

<sup>3</sup> Yunnan Key Laboratory of Wood Adhesives and Glue Products, Southwest Forestry University, Kunming, P.R. 650224, China

<sup>4</sup> V. Fierro, A. Celzard, IJL-ENSTIB, University of Lorraine, 27 rue Philippe Séguin, BP1041, 88051 Epinal cedex 9, France

Received June 1, 2014; Accepted August 13, 2014

**ABSTRACT:** Tannin/furanic foams, typically 95% composed of materials of natural origin such as prorobitenidin/profisetinidin tannins and furfuryl alcohol, are potential alternatives to oil-based synthetic foams such as phenol-formaldehyde, and polyurethane foams. This article describes the development of second generation tannin/furanic foams, which are not only formaldehyde free, but also use nonvolatile, nontoxic aldehydes. Both glyoxal and glutaraldehyde were tried to substitute formaldehyde in tannin/furanic foams. The physical properties of these new foams are described and discussed. It was found that glutaraldehyde can totally substitute formaldehyde during tannin/furanic foam preparation, but that glyoxal cannot. The optimized proportion to prepare such new foams is tannin:glutaraldehyde = 30:4 by weight. Formaldehyde-free glutaraldehyde-containing foams are open-celled and present good compression resistance and high thermal insulation.

**KEYWORDS:** Tannin/furanic foam, formaldehyde free, mechanical properties, thermal insulation

## 1 INTRODUCTION

Bioresourced polymeric foams based on commercial condensed tannins such as mimosa, pine and quebracho, namely tannin/furanic foams using formaldehyde, have already been developed [1-3]. These foams were found to be inexpensive and presented good compression resistance, high thermal insulation, fire resistance, etc. Moreover, tannin/furanic foams are composed of as much as 95% natural products. They are composed of two predominant raw materials: a) prorobitenidin or profidetinidin flavonoid tannin, namely a vegetable extract derived from tree bark or wood, and b) furfuryl alcohol, obtained through catalytic reduction of furfural, which is a natural derivative obtained by hydrolysis of carbohydrates from agriculture waste. They also constitute a promising alternative to phenol-formaldehyde foams and polyurethane foams in a variety of applications [4-10]. Tannin/furanic foams are

preferable with low content of formaldehyde or even formaldehyde free for both health and environmental reasons. To this purpose tannin/furanic foams with no aldehydes at all have been developed [11]; this kind of foam presents low thermal conductivity and is less brittle compared to tannin foam with formaldehyde. As tannins have much higher reactivity with formaldehyde than phenol [12], alternative but lower reactivity aldehydes could be envisaged for this application. Thus, glyoxal and glutaraldehyde were tried as an alternative route to substitute formaldehyde to prepare formaldehyde-free tannin/furanic foams. The physical properties of the obtained foams were also characterized and compared with formaldehyde-containing tannin/furanic foams.

## 2 MATERIALS AND METHODS

### 2.1 Materials

Commercial mimosa tannin (*Acacia mearnsii*, formerly *mollissima*, De Wildt) was supplied by SilvaChimica (S. Michele Mondovi, Italy). Mimosa tannin is

\*Corresponding authors: antonio.pizzi@univ-lorraine.fr;  
xiaojianzhou@hotmail.com

DOI: 10.7569/JRM.2014.634117

predominantly composed of prorobitenidins and contains more than 80% oligomers of A, B and C flavonoid units [13], as is represented in Figure 1, of which B is the predominant unit in this condensed tannin. Furfuryl alcohol (FA), glyoxal 40 wt% water solution (Gly) and glutaraldehyde 25 wt% water solution (Glu) were purchased from Acros Organics, Geel-Belgium. Diethyl ether was purchased from Sigma-Aldrich. Formaldehyde 37 wt% (Form) water solution was provided by Merck-Stuttgart OHG, Germany.

## 2.2 Foam Formulations and Preparation

The foam formulations are shown in Table 1. Water, furfuryl alcohol, Form (or Glu/ Gly), diethyl ether and tannin were first mixed under strong mechanical stirring. After 60 s, 65 wt% water solution of para-toluene-4-sulphonic acid (pTSA, catalyst) was stirred in for 20 s and the mixtures foamed and set. The foams were left for 5 days aging before testing according to predefined procedures [14]. The foams made using Form, Glu and Gly are labeled Std, GLY and GLU, respectively.

## 2.3 Measurement

### 2.3.1 Bulk density and mechanical property

Six samples were cut into  $30 \times 30 \times 15$  mm<sup>3</sup> specimens for the bulk density testing, defined as the weight of the bulk divided by its volume. Compression strength was measured with an Instron 4467 universal testing

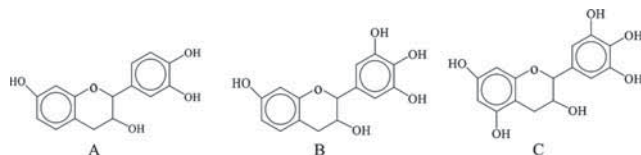


Figure 1 Mimosa tannin flavonoid units.

machine equipped with a 30 kN head at a constant load rate of 2.0 mm·min<sup>-1</sup>.

### 2.3.2 Viscosity

Viscosity was recorded with a Brookfield DV-II viscometer at the speed of 50 revolutions /min with rotor 27.

### 2.3.3 Scanning electron microscope (SEM)

Other foam samples were put into a freezer at  $-40^{\circ}\text{C}$  and then cut into  $5 \times 5 \times 4$  mm<sup>3</sup> specimens for observation in a Hitachi S 4800 Scanning Electron Microscope with a magnification of  $\times 20$ .

### 2.3.4 Thermal conductivity

Other foam samples were cut into  $100 \times 50 \times 30$  mm<sup>3</sup> and put into a vacuum oven for 1 day to drive away any residual blowing agent that could be possibly left in the foam. The thermal conductivity was measured by a Thermal conductivimeter FP2C (NeoTim) at room temperature with a sensor of 13.6 W, power of 0.04 W and testing time of 180 s.

### 2.3.5 MALDI-TOF mass spectrometry

The spectra of a tannin + furfuryl alcohol were recorded on a KRATOS Kompact MALDI AXIMA TOF 2 instrument. The irradiation source was a pulsed nitrogen laser with a wavelength of 337 nm. The length of a single laser pulse was 3 ns. The measurements were carried out using the following conditions: polarity-positive, flight path-linear, mass-high (20 kV acceleration voltage), and 100–150 pulses per spectrum. The delayed extraction technique was used by applying delay times of 200–800 ns. The samples were mixed with an acetone solution (10 mg/mL in acetone) of the matrix. As the matrix 2,5-dihydroxy

Table 1 Formulations used for mimosa tannin/furanic foam with different aldehydes.

Code	Water (g)	FA (g)	Form (g)	Glu (g)	Gly (g)	DE (g)	Tannin (g)	pTSA (g)
Std	6	10.5	7.4	—	—	1-5	30	11
GLY	6	10.5	—	—	7.4-16	3	30	11
F-Gly	6	10.5	4	—	4	3	30	11
GLU-12	0	10.5	—	12	—	3	30	11
GLU-16	0	10.5	—	16	—	3	30	11
GLU-20	0	10.5	—	20	—	3	30	11

benzoic acid was used. For the enhancement of ion formation NaCl was added to the matrix (10 mg/ml in water). The solutions of the sample and the matrix were mixed in the proportions 3 parts matrix solution + 3 parts polymer solution + 1 part NaCl solution, and 0.5 to 1  $\mu\text{L}$  of the resulting solution mix were placed on the MALDI target. After evaporation of the solvent, the MALDI target was introduced into the spectrometer. The dry droplet sample preparation method was used.

### 3 RESULTS AND DISCUSSION

#### 3.1 Foam Morphology

Both Std and GLU formulations foamed in 20 s after addition of pTSA catalyst and hardened into a foam after 3 mins. GLU-12 shrunk slightly at the end of foaming. GLY also foamed in 20 s, however, it markedly shrunk at the end of foaming. Photographs of GLU-15 and GLY are shown in Figure 2a. In the Std foam, 0.091 moles formaldehyde is added. If we take formaldehyde as a difunctional reagent, this is equivalent to saying that it presents 0.183 moles of reactive sites. However, there are only 0.061 moles of  $-\text{CHO}$  groups in Glu-12, which is not enough to crosslink the system well. Thus, its viscosity does not increase quickly enough for the foam to set simultaneously to foaming. The consequence of the two reactions, condensation and foaming, being out of phase lead to the observed shrinkage. Instead, Glu-16 and Glu-20, which contained sufficient aldehyde groups to have an effective level of crosslinking, did not show any shrinkage. GLY shrinkage is instead likely to be caused by a different mechanism: though the amount of GLY increased from 7.4 g to 16 g (the amount of  $-\text{CHO}$  groups increased from 0.128 mol to 0.255 mol), shrinkage did not disappear. Thus, glutaraldehyde appears to be a suitable aldehyde to totally replace formaldehyde in the preparation of mimosa tannin/furanic foams, while glyoxal does not.

By adding different amounts of diethyl ether, the density of GLU-16 can be controlled from 60 ~ 400  $\text{kg}\cdot\text{m}^{-3}$ . The microstructure of a typical glutaraldehyde foam is shown in Figure 2b.

#### 3.2 Reactivity of Tannin with Different Aldehydes

After the pTSA catalyst addition, the reaction starts. As the reaction proceeds, the viscosity should increase until a hardened resin or a foam is obtained. As the furfuryl alcohol self-condenses very rapidly once pTSA is added, only tannin and aldehyde were mixed to study

their reaction rates. Thus, 30 g tannin, aldehyde (Form, Gly or Glu) and 11 g pTSA were mixed together under strong stirring as shown in Table 2 and the viscosity increases were determined (Fig. 3).

From Table 2 and Figure 3, under the same condition, the viscosity of the mixtures ( $\eta$ ) and their increasing rate of the viscosity ( $I$ ) are in the following order:

$$\eta_{M1} \gg \eta_{M2} > \eta_{M3} \quad (1a)$$

$$I_{\text{Form}} \gg I_{\text{Glu}} > I_{\text{Gly}} \quad (1b)$$

The viscosity of the mixture with glutaraldehyde is 2–3 times higher than the mixture with glyoxal in the



Figure 2 (a) Photograph of glutaraldehyde foam and glyoxal foams; (b) SEM image of a typical glutaraldehyde foam.

Table 2 Formula to study the reactivity of tannin and different dialdehydes.

	Water	Tannin	Form	Glu	Gly	pTSA
M1	6	30	7.4	—	—	11
M2	0	30	—	16	—	11
M3	0	30	—	—	16	11

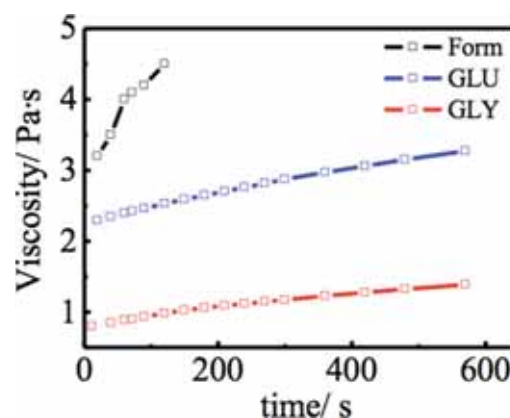


Figure 3 Viscosity curve of the mixtures of tannin and different aldehydes.

time range 0 s to 600 s (Fig. 3). This indicates that the relative reaction rates ( $R$ ) of mimosa tannin with the different aldehydes are:

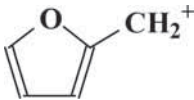
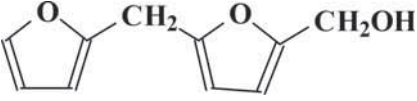
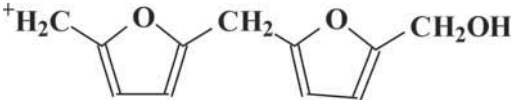
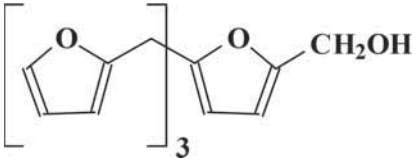
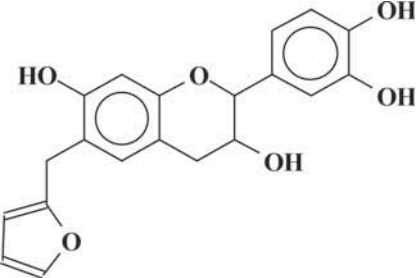
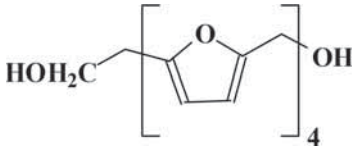
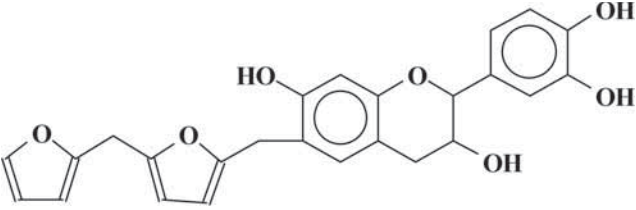
$$R_{\text{Formaldehyde}} \gg R_{\text{Glutaraldehyde}} > R_{\text{Glyoxal}} \quad (2)$$

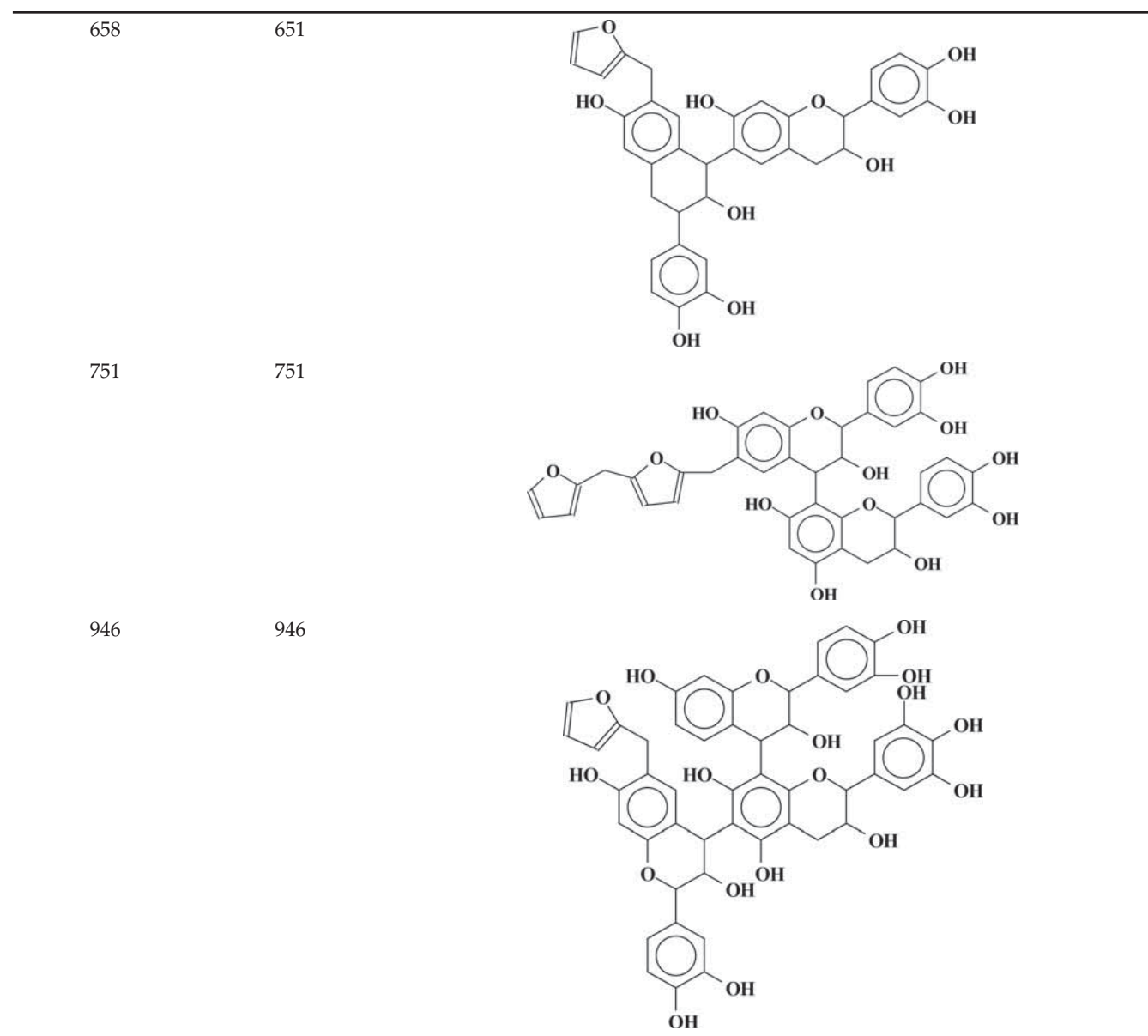
However, it must be pointed out that the reactions among tannin + furfuryl alcohol + aldehyde are complex [15], and involve several simultaneous and sequential reactions of the three materials. The reaction products of tannin + formaldehyde, tannin +

other aldehydes are already well known and identified [16,17]. Thus, a MALDI-TOF analysis of the reaction of mimosa tannin + furfuryl alcohol with the reaction stopped before gelling yielded the series of oligomers shown in Table 3.

Table 3 shows the different oligomers formed. All peak values are based on the MW of the species + 23 Da due to the  $\text{Na}^+$  of the NaCl matrix used. Both Figure 4a and b show peaks at 104 Da, 198/199 Da (Table 3), 215 Da, 365 Da and 397 Da, indicating that the self-condensation of furfuryl alcohol does indeed occur.

**Table 3** Oligomers identified by MALDI-TOF mass spectrometry in the reaction of mimosa tannin + furfuryl alcohol + formaldehyde before gelling.

Peak (Da)		Species
Experimental	Calculated	
104	103	
198/199	201	
215	215	
365	365	
375	376	
397	401	
459	457	



The most common flavonoid repeating units present in extracted mimosa tannins are fisetinidin, robinetinidin and delphinidin [13]. The peak at 375 Da is an oligomer formed by a fisetinidin monomer reacted with furfuryl alcohol, and at 658 Da the oligomer is formed by a fisetinidin dimer reacted with one furfuryl alcohol. The whole series of oligomers at 375 Da, 458 Da, 658 Da, 751 Da and 946 Da was identified as products of coreaction between flavonoid monomers, dimers and trimers characteristic of mimosa tannin with furfuryl alcohol and furfuryl alcohol prereacted oligomers.

For tannin/furanic/glutaraldehyde the reactions can be presented as in Scheme 1.

### 3.3 Compression Strength

Foam compression tests have been performed at 25°C. For clarity of presentation, only the results for four samples of Glu-16 are presented in Figure 5. For each sample, three domains can be distinguished: linear elastic (up to 10% strain, on average), long serrated plateau and densification. The long serrated plateau, see Figure 5a, typically ranging from 10% to 60% strain, originates from the coexistence of collapsed and uncollapsed zones. This is typical of a brittle foam undergoing successive cell wall fractures. Beyond the plateau, densification takes place and the stress rises sharply as complete densification begins. These features are

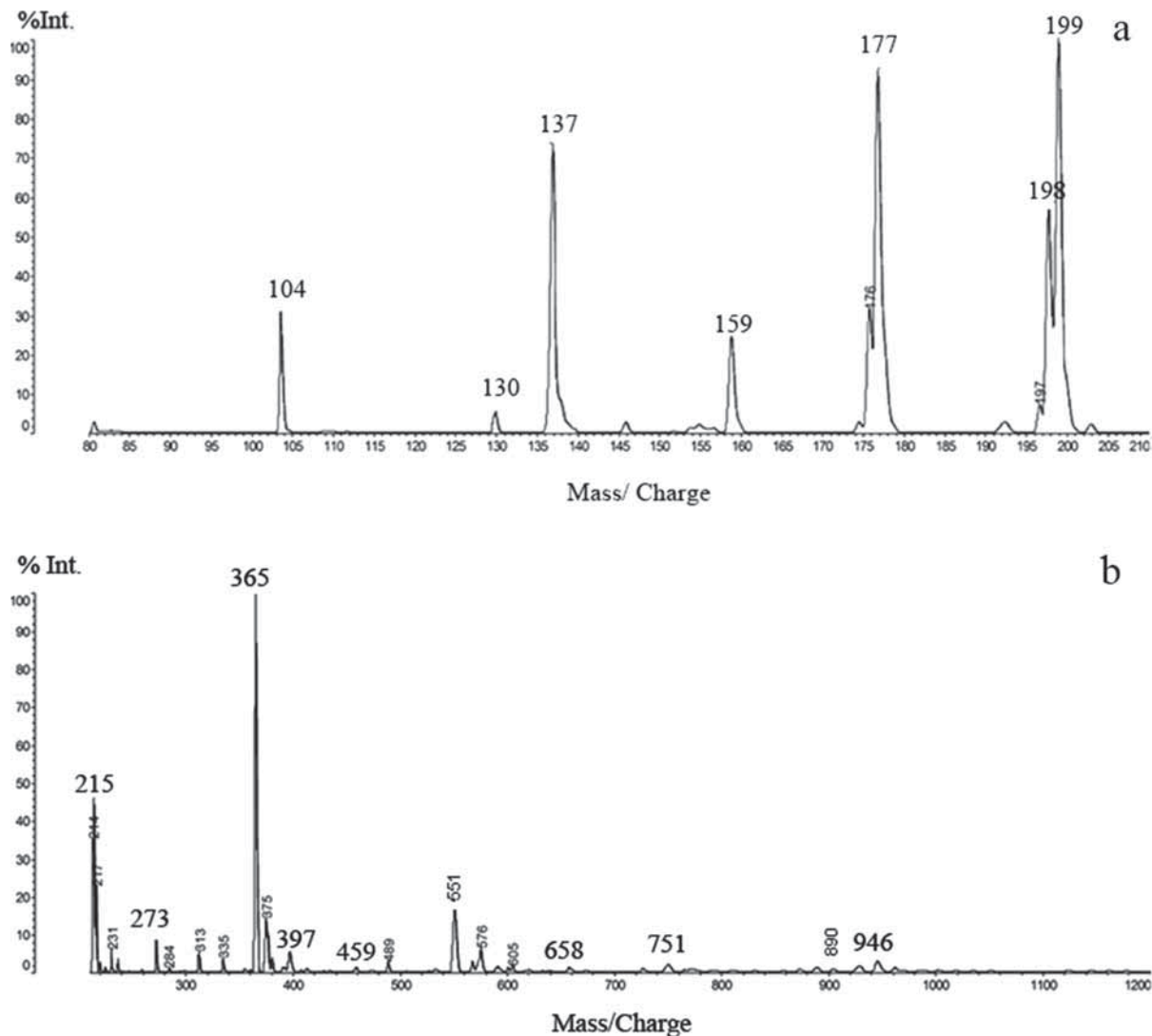


**Figure 4** MALDI-TOF peaks for mimosa tannin + furfuryl alcohol: (a) 80–210 Da range, (b) 210–1200 Da range.

also typical of phenol–formaldehyde foams [18–20]. As expected, higher density yielded higher compression strength.

The compression strength of the foams is derived from Figure 5a, and its relationship with bulk density is presented in Figure 5b. Figure 5b shows that GLU-16 foam is as strong as the Std foam. GLU-16 is found to be the one presenting the highest compression strength of the three GLU formulations. If less glutaraldehyde is added, like GLU-12, the resin is not crosslinked enough, resulting in a lower strength. However, considering that glutaraldehyde concentration in water is only 25%, to add more glutaraldehyde means to add more water, lowering the formulation solids content. When water evaporates, it will introduce defects into the finished foam, thus also causing GLU-20 to be weaker than GLU-16.

The relative density and compressive strength obey a power law [21–23],

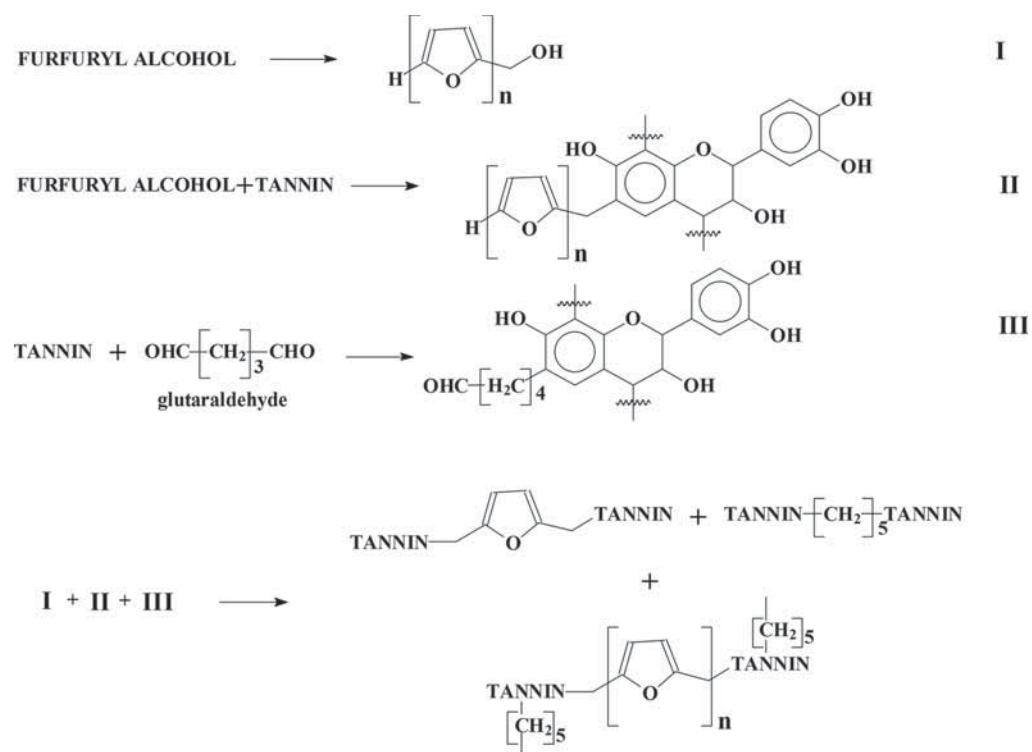
$$\sigma_{pl}^* \propto \sigma_{ys} \left( \frac{\rho^*}{\rho_s} \right)^a \quad (3)$$

where  $\sigma_{pl}^*$  is the compressive strength of the foam,  $\sigma_{ys}$  is the compressive strength of solid,  $\rho^*$  is bulk density,  $\rho_s$  is true density and  $a$  is constant. Fitting the results of GLU-16 in Figure 4b with Equation 3 yields:

$$\sigma_{pl}^* = 10^{-4.16} \times \rho^{*1.95} \quad (R^2 = 0.998) \quad (4)$$

### 3.4 Thermal Conductivity

Thermal conductivity of foams consists of four contributions: conduction through the solid,  $\lambda_s$ ; conduction



**Scheme 1** Proposed reaction scheme of tannin + furfuryl alcohol + glutaraldehyde.

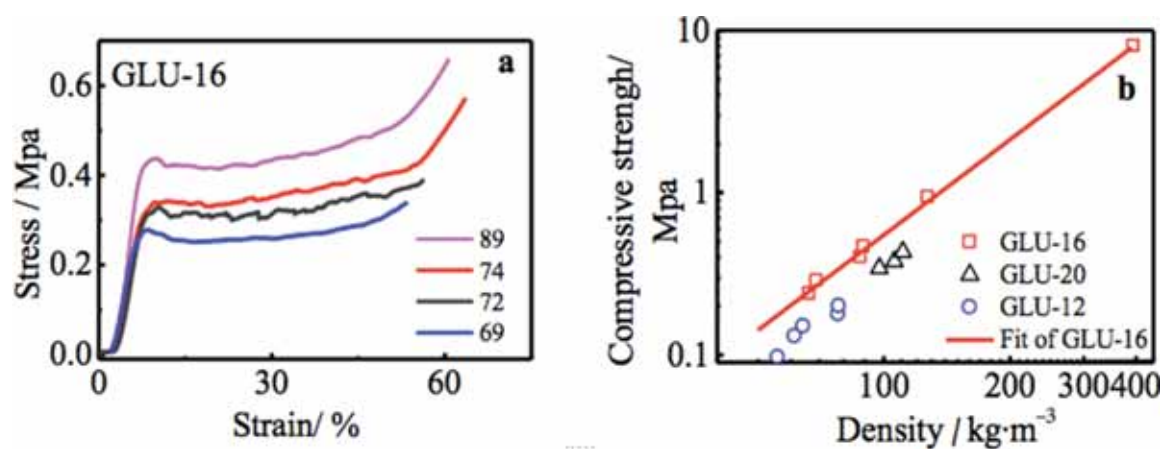


**Figure 5** (a) Stress-strain characteristics of a mimosa tannin/furanic/glutaraldehyde foam at different densities (89, 74, 72 and 69 kg/m<sup>3</sup>); (b) Compression strength of tannin/furanic foams with different amounts of glutaraldehyde in comparison to the Std formaldehyde foam.

through the gas inside of cells,  $\lambda_g$ ; convection within the cells,  $\lambda_c$ ; and radiation through the cell walls across the cell voids,  $\lambda_r$  [24,25]. The convection can be ignored when the diameter of cells is less than 10 mm [21], which is the case for the foams in this article. The thermal conductivity of second generation mimosa tannin/furanic foams has been measured, and the results are reported in Figure 6. The thermal conductivity of the foams with densities between 50 and 200 kg·m<sup>-3</sup> as a function of density present a linear relationship.

Fitting the thermal conductivity of GLU-16 as a function of its density yields the following linear regression equation:

$$\lambda^* = 0.0292 + 1.96 \times 10^{-4} \rho^* \quad (R^2=0.984) \quad (5)$$

As density increases, the porosity of the foam decreases, and the foam contains more solid and less air; hence this results in a gradual increase in thermal conductivity. Comparing the thermal conductivity of

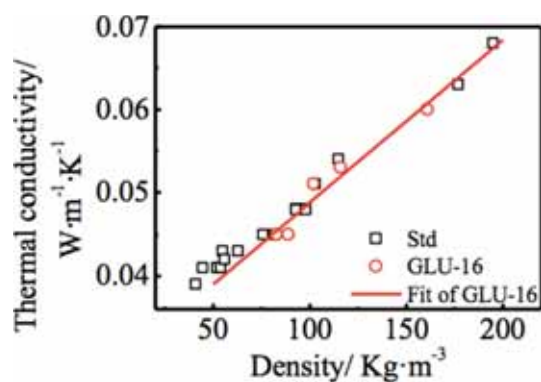


**Figure 6** Thermal conductivity of formaldehyde-free tannin/furanic/glutaraldehyde foams.

the Std and GLU-16 foams in Figure 5, the replacement of formaldehyde with glutaraldehyde did not bring an increase of thermal conductivity.

Moreover, as we can see from Figure 6, the thermal conductivity of the tannin/ furanic/glutaraldehyde foam is much lower than  $0.25 \text{ W}\cdot\text{m}^{-1}\cdot\text{K}^{-1}$ , a value which is usually considered to be the limit for insulating materials. This suggests that such a type of formaldehyde-free tannin/furanic foam presents excellent thermal insulation.

## 4 CONCLUSION

1. To prepare prorobinetinidin/profisetinidin type tannin/furanic foams, glutaraldehyde can be used instead of formaldehyde, but glyoxal cannot. These formaldehyde-free foams are open-celled.
2. Glutaraldehyde is more reactive with prorobinetinidin/profisetinidin type tannins such as mimosa than glyoxal.
3. When using glutaraldehyde, the best weight ratio to prepare the foam is tannin/glutaraldehyde = 30:4.
4. The tannin/furanic/glutaraldehyde foams have very low thermal conductivity, hence excellent insulation capabilities.
5. The tannin/furanic/glutaraldehyde foam has the same mechanical properties as tannin/furanic/formaldehyde foam, while being free of formaldehyde.

## REFERENCES

1. N.E. Meikleham and A. Pizzi, Acid- and alkali-catalyzed tannin-based rigid foams. *J. Appl. Polym. Sci.* **53**, 1547 (1994).
2. M.C. Basso, S. Giovando, A. Pizzi, M.C. Lagel, and A. Celzard, Alkaline tannin rigid foams. *J. Renew. Mater.* **2(3)**, 182–185 (2014).
3. V.K.Srivastava and A. Pizzi, Characterization and preparation of wood-furanic foams. *J. Renew. Mater.* **2(3)**, 201–206 (2014).
4. A. Celzard, W. Zhao, A. Pizzi, and V. Fierro, Mechanical properties of tannin-based rigid foams undergoing compression. *Mat. Sci. Eng. A-Struct.* **527**, 4438 (2010).
5. A. Celzard, V. Fierro, G. Amaral-Labat, A. Pizzi, and J. Torero, Flammability assessment of tannin-based cellular materials. *Polym. Degrad. Stabil.* **96**, 477 (2011).
6. X. Li, M.C. Basso, F.L. Braghiroli, V. Fierro, A. Pizzi, and A. Celzard, Chemical modification of tannin/furanic rigid foams by isocyanates and polyurethanes. *Maderas-Cienc. Tecnol.* **14**, 257 (2012).
7. X. Li, M.C. Basso, F.L. Braghiroli, V. Fierro, A. Pizzi, and A. Celzard, Tailoring the structure of cellular vitreous carbon foams. *Carbon* **50**, 2026 (2012).
8. X. Li, V.K. Srivastava, A. Pizzi, A. Celzard, and J. Leban, Nanotube-reinforced tannin/furanic rigid foams. *Ind. Crop. Prod.* **43**, 636 (2013).
9. M.C. Basso, A. Pizzi, and A. Celzard, Dynamic foaming behavior of polyurethane vs tannin/furanic foams. *J. Renew. Mater.* **1(4)**, 273–278 (2013).
10. M.C. Lagel, A. Pizzi, S. Giovando, and A. Celzard, Development and characterisation of phenolic foams with phenol-formaldehyde-chestnut tannins resin. *J. Renew. Mater.* **2(3)**, 220–229 (2014).
11. M.C. Basso, X. Li, V. Fierro, A. Pizzi, S. Giovando, and A. Celzard, Green, formaldehyde-free, foams for thermal insulation. *Adv. Mater. Lett.* **2**, 378 (2011).
12. A. Pizzi, *Chemistry and Technology*, pp. 56–77, Marcel Dekker, New York (1983).
13. H. Pasch, A. Pizzi, and K. Rode, MALDI-TOF mass spectrometry of polyflavonoid tannins. *Polymer* **42**, 7531 (2001).
14. G. Tondi and A. Pizzi, Tannin-based rigid foams: Characterization and modification. *Ind. Crop. Prod.* **29**, 356 (2009).
15. A. Pizzi, G. Tondi, H. Pasch, and A. Celzard, Matrix-assisted laser desorption/ionization time-of-flight structure determination of complex thermoset networks: Polyflavonoid tannin-furanic rigid foams. *J. Appl. Polym. Sci.* **110**, 1451 (2008).
16. A. Pizzi, H. Pasch, A. Celzard, and A. Szczurek, Oligomer distribution at the gel point of tannin-resorcinol-formaldehyde cold-set wood adhesives. *J. Adhes. Sci. Technol.* **27**, 2094 (2012).
17. A. Sauget, X. Zhou, and A. Pizzi, MALDI-TOF analysis of tannin-resorcinol resins by alternative aldehydes: Glyoxal and glutaraldehyde. *J. Renew. Mater.* **2(3)**, 186–200 (2014).
18. C. Gontier, A. Bouchou, and C. Vinot, A mechanical model for the computation of phenolic foams in compression. *Int. J. Mech. Sci.* **43**, 2371 (2001).
19. M.H. Ozkul and J.E. Mark, The effect of preloading on the mechanical properties of polymeric foams. *Polym. Eng. Sci.* **34**, 794 (1994).



20. H. Shen and S. Nutt, Mechanical characterization of short fiber reinforced phenolic foam. *Appl. Sci. and Manuf.* **34**, 899 (2003).
21. L.J. Gibson and M.F. Ashby, *Cellular Solids: Structure and Properties*, pp.180–182, Cambridge University Press, UK (1997).
22. W.S. Sanders and L.J. Gibson, Mechanics of BCC and FCC hollow-sphere foams. *Mat. Sci. Eng. A-Struct.* **352**, 150 (2003).
23. W.S. Sanders and L.J. Gibson, Mechanics of hollow sphere foams. *Mat. Sci. Eng. A-Struct.* **347**, 70 (2003).
24. M.A. Schuetz and L.R. Glicksman, A basic study of heat transfer through foam insulation. *J. Cell. Plast.* **20**, 114 (1984).
25. C. Venkatesan, G.P. Jin, M.C. Chyu, J.X. Zheng, and T.Y. Chu, Measurement of thermophysical properties of polyurethane foam insulation during transient heating. *Int. J. Therm. Sci.* **40**, 133 (2001).